Plant macrofossil and biomarker evidence of fen-bog transition and associated changes in vegetation

Tiina Ronkainen [a*], Erin L. McClymont [b], Eeva-Stiina Tuittila [c,d], MinnaVäliranta [a]

[a] *Environmental Change Research Unit (ECRU), Department of Environmental Sciences, PO Box 65, FI-00014 University of Helsinki, Finland*

[b] *Department of Geography, Durham University. South Road, Durham DH1 3LE, UK*

[c] *Current address: School of Forest Sciences, University of Eastern Finland, PO Box 111, 80101 Joensuu, Finland*

[d] *Peatland Ecology Group, Department of Forest Sciences, PO Box 27, FI-00014 University of Helsinki, Finland*

[*] Corresponding author. *E mail address*: tiina.m.ronkainen@helsinki.fi (Tiina Ronkainen)

1. Introduction

Peatlands can be divided into two main types; fens and bogs, with the main factor controlling the peatland type and the occurrence of species being the ecohydrology, i.e., the quantity and quality of water (Wheeler and Proctor, 2000; Økland et al., 2001). Fens are relatively shallow and they receive water and nutrients from the underlying and surrounding mineral soils, groundwater and atmosphere (Rydin et al., 2006). **Various** sedge species, forbs, minerotrophic Sphagna (e.g. *Sphagnum subsecundum* and *S. riparium*) as well as brown mosses such as *Warnstorfia* species **dominate fen habitats**. In contrast, due to effective peat formation and the consequential increase in **height**of the peat surface, bogs are nutrient poor as they receive water and nutrients only through precipitation, maintaining plants**,** including hummock Sphagna (e.g. *Sphagnum fuscum*), dwarf shrubs, lichens and true mosses (e.g. *Pleurozium schreberi* and *Polytrichum* spp.) (Rydin et al., 2006). **The** different environmental conditions in terms of the level of acidity, nutrient status and water table level means **that raised bog peats in boreal region** usually contain less-humified peat, while in groundwater-fed less acidic fen environments biomass decay is much faster and highly humified peat layers are formed (Moore et al., 2007).

Peatlands play an important role in atmospheric carbon cycling. Northern peatlands alone are estimated to store 547 (473-621) Pg organic carbon (Yu et al., 2010), yet, simultaneously peatlands are a natural source of CH_4 to the atmosphere (Matthews, 2000). As different peatland habitats and their vegetation, even within one peatland complex, have a vital role **in** the carbon budget of the peatland (e.g. Riutta et al., 2007), and the fact that bryophyte- and vascular plant- dominated communities differ in their CO_2 and CH_4 dynamics (Laine et al., 2007; Levy et al., 2012), it is important to be able to separate different habitats when reconstructing peatland dynamics back in time (Yu et al., 2013). Historical peatland habitats are preserved in peat layers as decomposed plant remains that form a key proxy when reconstructing the carbon budget of the peatland or historical climatic conditions (e.g. Barber et al.; 1998; Mauquoy et al.; 2002; Tuittila et al., 2007; Väliranta et al., 2007). Due to natural peatland succession **towards ombrotrophic conditions driven by peat height growth, minerotrophic (Frolking et al. 2010) fen peat layers are likely deposited under most of the** southern boreal raised bogs. Moreover, most of the high latitude peatlands are still the fen type of peatlands (e.g. Turunen et al., 2002) and in these environments the lack of identifiable plant remains may hamper palaeoecological and -climatological reconstructions.

Recently organic geochemistry analyses have shown that the lipid fractions of plants contain biomarkers for identifying different plant species and plant groups from peat archives.

Studies on bog peat environments have shown that plant group-specific chemical compounds can be applied to identify fossil plants or plant groups from peat (e.g. Avsejs et al., 2002; Bingham et al., 2010; Jia et al., 2008; McClymont et al., 2008; Xie et al., 2000). The most widely analyzed compounds have been the *n*-alkanes: for instance, the difference between concentrations of mid chain length (*n*-C_{23} and *n*-C_{25}) and long chain length (*n*-C_{29} and *n*-C_{33}) *n*-alkanes have been used to separate contributions of *Sphagnum* and vascular plant species in the peat (e.g. Andersson et al., 2011; López-Días et al., 2010; Nichols et al., 2006; Ortiz et al., 2011; Pancost et al., 2002; Ronkainen et al. 2013; Vonk and Gustafsson, 2009). Furthermore, the *n*-C_{23}/*n*-C_{25} alkane ratio has been successfully used in tracking changes in *Sphagnum fuscum* abundance in a peat section from Finland (Bingham et al., 2010).

Thus far, in environmental reconstructions the biomarker analyses have focused on bog peats and plants typical to bogs. However, a pertinent question remaining is whether such plant-specific biomarkers could also provide information about the past plant assemblages in fen environments characterized by highly humified peat, where macrofossil remains are heavily degraded and thus essential information for environmental reconstruction is lost. Some previous studies have applied "bog" biomarker analyses throughout the peat profile, including the fen peat section underlying the bog peat section (e.g. Andersson and Myers 2012; Andersson et al., 2011). However, our recent study of the *n*-alkane concentrations, *n*-alkane ratios, and sterol distributions of moss and vascular plant species typical to fen habitats **showed** differences between some of the biomarker distributions between plant species characteristics to bogs and fens (Ronkainen et al., 2013). **As in** previous studies on bog plants (Baas et al., 2000; Ficken et al., 1998; Nichols et al., 2006; Pancost et al., 2002) fen *Sphagnum* species were also dominated by mid-chain *n*-alkanes and the above ground parts of fen vascular plants by long-chain *n*-alkanes. However, results showed similarity in the dominating *n*-alkanes of *Sphagnum* species and below-ground parts of sedges in studied fen plants and thus, applying *n*-alkane ratios from bog plants to fen peats could result in incorrect interpretations about the actual proportions of these plant groups in peat (Ronkainen et al., 2013). Similar mid-chain *n*-alkane distributions in vascular plant roots were also reported by Huang et al. (2011). The similarity of *n*-alkane distributions in *Sphagnum* species and vascular plant below-ground parts suggest that the *n*-alkane ratios that have predicted different plant groups in bog environments relatively well (e.g. Andersson et al. 2011; Bingham et al., 2010) may not be directly applicable to interpret past habitats in environments where sedges dominate and sedge roots form an important peat component. One potential way to overcome this problem could be to combine the distributions of plant group-specific *n*-alkanes, *n*-alkane ratios and sterols, if present, when analyzing the biomarker data (Ronkainen et al., 2013). The degradation of the plant matter and their chemical compounds could impede detection of especially sterols from the fen-bog transition and fen environment, where the peat **is usually** highly humified. The level of organic matter decomposition can be studied by comparing the variations in C/N ratio and the amount of total organic carbon (TOC) through the peat section (Kuhry and Vitt 1996) In addition, the ratio between 5α(H)-stanols and Δ^5-sterols can be used to infer the rate of sterol degradation because 5α(H)-stanols are known as degradation products of the Δ^5-sterols (McClymont et al., under review). A high 5α(H)-stanols and Δ^5-sterols ratio is related to anoxic conditions, shallow water table level and high rate of degradation (Bertrand et al., 2012; McClymont et al., under review). The level of degradation can also be estimated by *n*-alkane CPI value, where high CPI value is linked to high amount of well-preserved plant material (Andersson and Meyers 2012; Xie et al., 2004).

In this study we analyzed fossil plant and biomarker compositions of two peat sections. We concentrated on the fen-bog transition phase where the plant composition is known to change (e.g. Dudová et al., 2013; Loisel and Yu, 2013; Salojärvi et al. in prep.; Tuittila et al. 2013). We aimed to investigate (1) if biomarkers can be applied to distinguish fen and bog environments, and (2) if plant-specific biomarkers can be identified from fen peat. For this we applied plant macrofossil analysis to examine the past plant compositions from the same subsamples from which the selected organic geochemical-analyses were **obtained**.

2. Material and methods

2.1. Sampling

Two peat sections (SJ5 and SJ6) were collected from two closely located peatlands in Siikajoki (64°45´N, 24°42´E) located near west coast of Gulf of Bothnia, Baltic Sea in the mid-boreal bio-climate zone in Finland (Fig. 1). A chronosequence of terrestrial ecosystems from coast to inland have been created by the postglacial isostatic rising, and along the sequence peatlands alternate with sand dunes and glaciofluvial ridges (Tuittila et al., 2013). We have previously studied vegetation, microbial communities and carbon dynamics along a transect of seven mires (SJ0 to SJ6) (e.g. Leppälä et al. 2011a,b, Laine et a. 2011, Tuittila et al. 2013, Larmola et al. *in press*). In this study we concentrated on the two oldest sites of the transect, and in particular on their sediment sections where fen-bog transition occurred, from which historical plant communities had already been studied (Tuittila et al. 2013). Site SJ5 represents a peatland stage where the fen-bog transition is still partly in progress; vegetation is a mosaic of wet fen communities and drier bog communities, the average water table level is at 12 cm below moss layer surface and the basal age of the peatland is 2520 (±20) years BP. The peat core was taken from a drier surface dominated by lawn species (*S. magellanicum*). Site SJ6 is already a true bog with vegetation formed by hummock Sphagna and dwarf shrubs, average water table level 32 cm below moss surface and the basal age of 3000

years (both cores basal ages are extrapolated from known land-uplift rate). The top section of the peat core was dominated by hummock species (*S. fuscum)*, More detailed site descriptions can be found in Leppälä et al. (2011), and Tuittila et al. (2013). The sampling depth for SJ5 was 6 – 150 cm and for SJ6 0 – 100 cm. Both cores were cut into 2 cm sample slices and analyzed with a varying down-core resolution by focusing on the fen-bog transition.

2.2. Plant macrofossil analyses

Plant macrofossil sample volume was 5 cm^3. Samples were rinsed under running water using a 140-µm sieve **and no chemical treatment was needed**. Remains retained on a sieve were identified **and the percentage in volume of constitute within the total composition of the sample was visually estimated by** using a stereomicroscope **(magnification of 10x) (e.g. Speranza et al., 2000; Mauquoy et al., 2002**) If the proportion of bryophytes exceeded 10 % of the total sample volume a high power light microscope was used to identify bryophyte species and to count proportions for different bryophyte species. Also, the proportion of unidentified organic matter (UOM) from samples was estimated (cf. Väliranta et al., 2007 and references therein).

2.2. Solvent extraction

Peat samples for solvent extraction were freeze dried and ground following the same procedure in Ronkainen et al. (2013). Lipids were extracted from ca. 0.2 g of samples using repeated ultrasonication (20 min) with 6 ml CH_2Cl_2/MeOH (3:1, v/v). Samples were saponified with 0.5 M methanolic (95%) NaOH for 2 h at 70 °C and the neutral lipids were extracted using hexane. The neutral lipids were further separated into apolar and polar compounds using activated Al_2O_3 columns, eluting with hexane/CH_2Cl_2 (9:1, v/v) and

CH_2Cl_2/MeOH (1:2, v/v), respectively. Prior to analysis using gas chromatography (GC) and GC-mass spectrometry (GC-MS), the polar fractions were derivatised using bis(trimethylsilyl)trifluoroacetamide (Sigma Aldrich).

2.3. GC-MS

Apolar and polar fractions were analyzed using GC-MS with a gas chromatograph equipped with flame ionisation detection (GC-FID) and split/splitless injection (280 C). Separation was achieved with a fused silica column (30 m x 0.25 mm i.d) coated with 0.25µm 5% phenyl methyl siloxane (HP-5MS), with He as carrier gas, and the following oven temperature program: 60 – 200 °C at 20 °C/min, then to 320 °C (held 35 min) at 6°C/min. The mass spectrometer was operated in full scan mode (50-650 amu/s, electron voltage 70eV, source temperature 230 °C). Compounds were assigned using the NIST mass spectral database and comparison with published spectra (e.g. Goad and Akihisa, 1997; Killops and Frewin, 1994). Quantification was achieved through comparison of integrated peak areas in the FID chromatograms and those of internal standards of known concentration (5-α-cholestane for apolars and 2-nonadecanone for polars). Biomarker concentrations were normalized to total organic carbon (TOC) content and are presented here as concentration per g TOC, so that samples with different extent of degradation become comparable (Meyers 2003; Ortiz et al., 2010). Total organic C and N_2 were measured by the CHN elemental analysis, where 1-2 mg dried and ground sample was combusted at 950°C with He as a carrier gas. The reduction of the combustion gases **was** carried out in a separate furnace, and separated into individual components on a temperature programmed desorption column and fed into a thermal conductivity detector. Results were computed as concentrations of C and N_2 from the detector signal.

2.4. Statistical analysis

We applied multivariate analyses to study the variation within the plant macrofossil and biomarker data (triterpenoids, sterols, stanols, *n*-alcohols (C_{20}-C_{28}) and *n*-alkanes (C_{20}-C_{35}) (µg/g TOC), and *n*-alkane ratios**, see the supplementary data 2**). For the analyses we combined macrofossil and biomarker data from both cores by depth.

We first quantified separately the variation in macrofossil plant species and biomarkers within the peat profiles by unconstrained (indirect) gradient analysis. **For macrofossils we used detrended correspondence analysis (DCA) where detrending was conducted by segments. All identified macrofossils were included in the analysis, with down-weighting of rare species. Macrofossil data was log transformed. For biomarkers we used principal component analysis (PCA) with centered and standardized data. No exclusion of biomarkers due low concentrations was done.** Secondly, for the biomarker data we conducted redundancy analysis (RDA), a constrained (direct) gradient analysis, to test if the variation in biomarkers in the peat profiles correlates with the variation in macrofossil data. For the analysis we applied the sample scores along the first and second macrofossil DCA axes as explanatory variables. **Similarly to PCA the biomarker data was centered and standardized. All constrained axes were tested with unrestricted Monte Carlo permutation (number of permutations 499).** Multivariate analyses were conducted by using Canoco for Windows 4.52 (ter Braak and Smilauer, 2002). **The correlation of the ten most significant biomarkers identified in RDA with** depth and UOM was analysed with Pearson two-tailed correlation using SPSS PASW statistics 18.

We applied TWINSPAN (Two Way INdicator SPecies ANalysis, Twinspan for Windows 2.3) to define groups of macrofossils and biomarkers that share a similar abundance peak in the peat profile . For the analysis we rescaled the abundances for each macrofossil and biomarker from 0 to 1 by setting the highest abundance of each unit to 1 and calculating other values as a percentage of the highest abundance of the unit. In the analysis we used five cut levels (0.0, 0.2, 0.4, 0.6 and 0.8) of abundance and two division levels, which determines the maximum level of recursive splitting for samples and for species (Hill and Šmilauer, 2005). The statistical analyses allow us to assess the relationship of the biomarkers to the macrofossil record and to determinate if macrofossils and biomarkers can separate different environmental habitats as individual or rather as combined proxies.

3. Results

3.1. Macrofossil analyses

Sub-fossil plant assemblages revealed clearly the vegetation succession from fen to bog stage (Fig. 2). Core SJ5 showed dominance of higher plants (*Menyanthes trifoliata, Scheuzeria palustris, Equisetum* sp.) in the earliest stage of the succession (150 – 100cm). In core SJ6 these plants were present but they did not dominate (100 – 80 cm). In both of the studied cores the transition from fen to bog environment is **both identified and induced** by the appearance of *Eriophorum* sp. and sedge roots followed by a distinctive occupation of *Sphagnum* mosses at the depth of 40 – 20 cm in SJ5 and 75 – 55 cm in SJ6.

The DCA for macrofossil data (cores SJ5 and SJ6 combined) sub-divided the peat samples into three different groups: fen species (SJ5 150 – 30 cm and SJ6 98 - 62 cm), lawn species (SJ5 26 – 6 cm), and hummock species (SJ6 60 – 0 cm). The first axis describing the fen-bog gradient explained **28** % (eigenvalue **0.5298**) of the variation in the data and the second axis describing the moisture gradient on bog explained **18** % (eigenvalue **0.3491**) of the variation (Fig. 3).

3.2. Biomarker analyses

3.2.1. Apolar fraction

Figures 4a and 4b show the distribution of *n*-alkanes in both peat cores (SJ5 and SJ6). In both cores, there is up-core variation in both overall *n*-alkane concentration and the chain-length of the dominant *n*-alkane. *n*-C_{27} dominated the bottom layers (150 – 36 cm) of SJ5, excluding layers 130 – 110 cm which were dominated again by *n*-C_{23} and *n*-C_{25} alkanes, while he uppermost layers (32 – 0 cm) were mainly dominated by *n*-C_{23} and *n*-C_{25} alkanes. In the deepest layers (100 – 60 cm) in core SJ6, the dominant *n*-alkane alternated between *n*-C_{23}, *n*-C_{29} and *n*-C_{31}. The middle layers (60 – 40 cm) were dominated by *n*-C_{25} whereas the uppermost layers (30 – 0 cm) of core SJ6 were dominated by the *n*-C_{31} alkane. Different *n*-alkane ratios showed changes along the depth in both cores (Fig. 5). In core SJ5 the ratios *n*-C_{23}/*n*-C_{27}, *n*-C_{23}/*n*-C_{29}, *n*-C_{31}/*n*-C_{27} and *n*-C_{31}/*n*-C_{29} showed differences along the core, separating the top and the bottom layers apart; all ratios being higher than 1 in top 25 cm. For core SJ6 several ratios were able to separate the top and bottom layers apart e.g. *n*-C_{23}/*n*-C_{25} and *n*-C_{25}/*n*-C_{23} indicated changes happening at 62 cm (Fig 5).

The distribution of the detected triterpenoids along the cores was similar for all compounds. In core SJ5 at depths 42 – 30 cm the maximum concentrations of taraxer-14-ene (ca. 60 – 720 µg/gTOC), and taraxast-20-ene (ca. 50 – 500 µg/gTOC) were recorded. Squalene was identified only in upper layers, peaking at 30 cm (30 µg/gTOC). In core SJ6 at depths 80 – 66 cm the maximum concentrations of taraxer-14-ene (260-1050 µg/gTOC) and taraxast-20-ene (500 – 1800 µg/gTOC) were recorded. Concentration of squalene was highest at 10 cm ca. 140 µg/gTOC, downcore the concentration was ca. 10 µg/gTOC (Fig 6). The highest concentrations of taraxer-14-ene and taraxast-20-ene coincided with high counts of sedge roots and UOM in the middle layers of both cores (Figures 2 and 6).

3.2.2. Polar fraction

The most abundant sterols found from both cores were: brassicasterol [(22*E*)-ergosta-5,22-dien-3β-ol],campesterol [campest-5-en-3β-ol], stigmasterol [(24*E*)-stigmasta-5,22-dien-3β-ol], and β-sitosterol [(3β)-stigmast-5-en-3-ol]. The associated stanols of these sterols were also detected: campestanol [24-methyl-5α-cholestan-3β-ol], 22E-stigmastanol [(24-ethyl-5α-cholest-22-3β-ol)] and 3-stigmastanol [(24-ethyl-5α-cholestan-3β-ol)]. In core SJ5 the concentration of brassicasterol was highest (ca. 150 µg/gTOC) at 50 – 30 cm; below and above this depth the concentration was less than 50 µg/gTOC, although concentrations increased in the uppermost 6 cm (80 µg/gTOC). The concentration of campesterol was also high in the uppermost 6 cm of core SJ5, reaching concentrations of ca. 2000 µg/gTOC. Between 50 – 30 cm depth the concentration of campesterol was ca. 500 – 1000 µg/gTOC, and elsewhere in the core the concentration was ca. 100 – 470 µg/gTOC. Stigmasterol in core SJ5 had similar concentrations and pattern as campesterol, and whilst β-sitosterol also followed this same pattern the concentrations were significantly higher, reaching a maximum of ca. 12 000 µg/gTOC at 30 cm depth (Fig. 6).

In core SJ6 the concentration of brassicasterol was higher than in core SJ5, it increased towards the top of the core with highest concentration at top 30 cm (200 – 500 µg/gTOC). The concentration of campesterol in core SJ6 was the highest at depths 80 – 60 and 0 cm (ca.1250 – 1700 µg/gTOC). Also stigmasterol peaked at 62-60 cm (1300 µg/gTOC) and at 0 cm (1900 µg/gTOC). The concentration of β-sitosterol was higher in core SJ6, peaking at 72 cm (20 000 µg/gTOC), elsewhere concentration varied between 2500 and 10 000 µg/gTOC. Tocopherol-α [(2R)-2,5,7,8-Tetramethyl-2-[(4R,8R)-(4,8,12-trimethyltridecyl)]-6-chromanol] was found only from the lowermost layers of core SJ6. In both cores all stanols, campestanol, 22E-stigmastanol and 3-stigmastanol, were identified from bottom to upwards at all layers until 10 cm in SJ5 and at 40 cm in SJ6 (Fig. 6).

In core SJ5 the concentration of phytol [(3,7,11,15-tetramethylhexadec-2-en-1-ol] was highest at 50 cm depth (ca. 2500 µg/gTOC), and the overall concentration decreased towards the top layers. In core SJ6 the concentration of phytol was highest in top layers, 60 – 0 cm, ca. 400 – 1200 µg/gTOC. Before 66 cm, phytol concentration was less than 400 µg/gTOC. The *n*-alcohol distribution in both studied cores did not vary substantially. In core SJ5 *n*-C_{22}-ol dominated depths 150, 120 and 100 – 6 cm, *n*-C_{24}-ol dominated depths 140, 130 and 110 cm, and *n*-C_{28}-ol dominated depth 70 cm. In core SJ6 *n*-C_{22}-ol dominated depths 100 – 50 cm, whereas *n*-C_{24}-ol dominated the uppermost 40 cm.

3.2.3. Statistical analyses of biomarkers

The PCA for biomarkers **produced** groups**, similar to the** DCA for macrofossils. However, when the biomarker RDA was performed (Fig.7), where sample scores from macrofossil DCA were used as explanatory variables, the biomarker distribution of the two peat profiles correlated significantly with their macrofossil compositions (pseudo F = 9.2, *p*-value = 0.002). RDA resulted in three groups similar to macrofossil DCA: fens (SJ5 150 – 30 cm and SJ6 98 – 62 cm), lawn (SJ5 26 – 6 cm), and hummock (SJ6 60 – 0 cm; Fig. 3). Biomarkers whose concentrations decreased in association with the shift from fen to bog habitat were the *n*-alkanes *n*-C_{20}, *n*-C_{22}, *n*-C_{24}, *n*-C_{26}, *n*-C_{27}, *n*-C_{28} and stanols. Markers for the top layers of core SJ5 (lawn) were e.g. the *n*-alkane ratios *n*-C_{23}/*n*-C_{27} and *n*-C_{31}/*n*-C_{29}, and for the top core of SJ6 (hummock) were e.g. *n*-C_{25}, *n*-C_{29}, and *n*-C_{28}-alcohol. The ten best-fitted biomarkers from **the** RDA are shown in figure 8. In core SJ5 *n*-alkanes *n*-C_{22}, *n*-C_{24}, *n*-C_{25}, *n*-C_{26}, *n*-C_{27} correlated positively and 22E-stigmastanol negatively with depth, and only *n*-C_{25}, *n*-C_{27}, *n*-C_{29} correlated with UOM. In core SJ6 most of the *n*-alkanes correlated positively with UOM and depth, with *n*-alkane concentrations decreasing towards top layers (Fig 8).

The first division of the TWINSPAN separated macrofossils from the top part of core SJ5, i.e. lawn species with urs- 12-ene from the rest of the samples (Table 1). The second division divided the rest of the data hummock species and biomarkers: (1) *S. fuscum* and shrub leafs with C_{27} *n*-alcohol, C_{34} *n*-alkane, and squalene, and (2) fen species and biomarkers: brown-mosses, sedge-roots, *Equisetum* sp., *Sch. palustris* and *M. trifoliata* together with biomarkers: 22E-stigmastanol, *n*-C_{35} and urs- 12-ene.

3.2.4. Degradation measures

In both cores **a** high amount of UOM corresponded to the fen-bog transition zone (SJ5: 30 – 20 cm and SJ6: 75 – 55 cm). In these layers 20-55 % of the plant macrofossil material was unidentified. In contrast, total organic carbon (TOC) showed little variation and stayed around 50 % throughout both of the cores (Fig 9). There was a clear up-core increase in the C/N ratio in both cores at the fen-bog transition. The most notable increase of the carbon preference index (CPI; e.g. Andersson et al. 2012) of *n*-alkanes also occurred during the transition. The ratio of 5α(H)-stanols/ Δ^5-sterols (Bertrand et al. 2012) decreased towards the top layers in both cores and was last detected in SJ5 at 10 cm and in SJ6 at 40 cm depth.

3. Discussion

Our results suggest that, statistically, individual biomarkers predict the fossil plant species composition rather poorly, in support of observations from previous studies (e.g. Andersson 2012; Ficken et al., 1998; Pancost et al., 2002) that recommended that biomarkers should be used as a complementary proxy. When we applied the combined data i.e. biomarkers together with macrofossils as explanatory variables a clear correlation between biomarkers and fossil plants was detected and the biomarkers succeeded in describing three different environments: bog hummocks and lawns, and fens (Fig. 7).

Previous studies have identified the high concentrations of n-C_{23} and n-C_{25} and high ratios of n-C_{23} to n-$C_{25,}$ n-C_{29} and n-$C_{31,}$ to be characteristic to hummock *Sphagnum*-species, whereas taraxer-14-ene, taraxas-20-ene, n-C_{31}, and the ratio of n-C_{31}/n-C_{33} to *Ericaceae*-species (e.g. Bingham et al., 2010; McClymont et al., 2008; Nichols et al., 2006; Nott et al. 2000; Pancost et al., 2002). In contrast, the study here shows that the statistically significant biomarkers for bog hummock species, *S. fuscum*, *S. angustifolium* and *Ericaceae* roots and leafs were n-C_{24}-ol, n-C_{26}-ol, n-C_{28}-ol, n-C_{25} and n-C_{29} (Fig 7). These compounds were particularly effective in identifying the difference between bog and fen zones (Figures 7 and 8). However, the visual comparison between the biomarker concentrations and palaeobotanical assemblages supports the previous works that **has** linked certain plant groups with certain biomarker distributions; for example in core SJ6 the uppermost layers were dominated by n-C_{31}, which is an indicator of *Ericaceae*-species whose macrofossils were also present. However, the triterpenoids and sterols associated with *Ericaceae*-species (e.g. Pancost, 2002) were not detected. Although *S. fuscum* dominated the whole hummock bog peat section (SJ6) the concentration of n-C_{25} was **exceeded** by n-C_{31} when descending from 0 cm to 40 cm, but the low ratio of n-C_{23}/n-C_{25} (< 1) indicate**s** a dry *Sphagnum*- dominated environment**,** as suggested by Bingham et al. (2010). In core SJ5, similar low n-C_{23}/n-C_{25} ratios were detected in layers dominated by sedge roots, which agrees with Ronkainen et al. (2013), whose data showed this ratio to correspond both with sedge below-ground parts and *Sphagnum* mosses. However, in core SJ6 the depths that were dominated by sedge roots (100 – 66 cm) have a higher n-C_{23}/n-C_{25} ratio than comparable layers in core SJ5 (100 – 40 cm) (Fig.5). These results support the conclusion of Ronkainen et al. (2013) who suggested that the application of bog biomarkers to fen environments may be complicated by the similar signatures of *Sphagnum* mosses and sedge roots.

A recent study showed that in general the most reliable proxy for *Sphagnum* mosses in peats are the *n*-alkane ratios *n*-C_{23}/*n*-C_{27} or *n*-C_{23}/*n*-C_{29} (Bush and McInerney, 2013). When studied visually rather than through the statistical analysis our results showed that SJ6 top peat layers (60 – 0 cm) dominated by *S. fuscum* were separated from the rest of the layers by low *n*-C_{23}/*n*-C_{29} ratio (< 0.5). The statistically significant ratio *n*-C_{23}/*n*-C_{27} (< 1.5) described core SJ5 top layers (36 – 0 cm) that were dominated by *S. magellanicum* and *S. papillosum*. Other statistically significant biomarkers describing the uppermost layers of the core SJ5 with lawn habitat were *n*-C_{31}/*n*-C_{27} and *n*-C_{31}/*n*-C_{29} (Fig.7 and 8). The *n*-alkanes that dominated the lawn layer with *S. magellanicum and S. papillosum* were *n*-C_{23}, *n*-C_{25} and *n*-C_{31}, which agree with Bingham et al. (2010). Consistent with the fact that lawns are relatively wet microhabitats when compared **with** hummocks, the previously suggested *n*-C_{23}/*n*-C_{25} and *n*-C_{23}/*n*-C_{31} ratios that should describe dry bog environment (Bingham et al. 2010) did not describe the wetter lawn environment.

In both cores the fen layers beneath bog peat consisted mainly of vascular plant remains, e.g. *M. trifoliata*, *Sch. palustris*, *Equisetum* spp. and sedges. These plants are usually dominated by odd-over-even long-chain *n*-alkanes (Fig. 2) and this was at least partly shown by RDA that grouped the mid- and long-chain *n*-alkanes C_{20}, C_{21}, C_{22}, C_{24}, C_{26}, C_{27} and C_{28} as well as three stanols as fen peat biomarkers (Fig.7). Bush and McInerney (2013) stated that *n*-C_{29} and *n*-C_{31} should not be used as general proxies for grasses and woody plants, as these two compounds are highly variable and are overlapping between these groups, but that by differences in mid-chain and long-chain *n*-alkanes *Sphagnum* mosses could be separated from them. Our results partly agree with this. In both of the studied cores the macrofossil records indicated the transition zone from fen to bog stage (SJ5; 30 – 20 cm, SJ6; 75 – 55 cm) distinctively. In core SJ5, the biomarker record indicates that the fen-bog transition is characterized by a shift from long-chain *n*-alkanes (C_{27}) to mid-chain *n*-alkanes (C_{23}) at depth 36 cm. Yet, in core SJ6 such a clear change is not visible.

In our study of modern fen species, we found that sterols such as lupeol [5α-lup-20(29)-en-3β-ol], obtusifoliol [4α,14α-dimethyl-5α-ergosta-8,24(24^1)-dien-3β-ol] and gramisterol [4α-methyl-5α-ergosta-7,24(24^1)-dien-3β-ol] showed potential to yield information about the abundance of sedge roots and mosses (Ronkainen et al., 2013). Even though sedge root remains and mosses were present in the studied peat, the above mentioned group-specific sterols were not detected and only brassicasterol, campesterol, stigmasterol, β-sitosterol that are common to most plant species were found from fossil peat material. We attribute this absence of the plant-specific sterols is due to degradation of these compounds (Lehtonen and Ketola 1993) given that their concentrations in fen plants was rather low (Ronkainen et al., 2013), and we conclude that appearance of stanols (Fig 6) indicates degradation of organic matter since deposition (cf. McClymont et al., under review). In both cores the fen-bog transition and the layers below the transition were characterized by the presence of stanols and it seems that especially the 5α(H)-stanols/Δ^5-sterol ratio, which is related to anoxic conditions and decay of plant material (Bertrand et al., 2012; McClymont et al. under review) is a strong marker for degradation, and changes in the ratio were consistent with degradation measures presented here (Fig 9). Similarly to Andersson and Meyers (2012), the CPI value increases up-core in both of the studied cores, indicating better preservation of organic matter at the top layers and a progressive degradation down core. In both cores CPI reaches its minimum right below the transition layer, almost simultaneously where the C/N ratio decreases to its minimum. In both cores the amount of UOM is clearly higher at and below the fen-bog transition than in the bog peat layers. Changes in the degradation measures might indicate that drier periods with lower water table level triggered the fen-bog transition **(Hughes and Barber, 2003; Hughes, 2000),** resulting in accelerated plant litter decay. This interpretation would correspond to McClymont et al. (under review) results where high 5α(H)-stanols/Δ^5-sterol ratio occurred simultaneously with low water table level. Also, around the fen-bog transition layer the concentrations of sterols and triterpenoids were high in the peat, while the dominating macrofossils were sedge roots and other parts of sedges. Previous studies have stated that sterol and triterpenoid concentrations are higher in vascular plants than mosses (e.g. Pancost et al., 2002; Ronkainen et al., 2013). The results presented here support this interpretation, and suggest that these compounds originate from vascular plants. This result is potentially important because high proportions of highly decomposed organic matter hampers reliable environmental reconstructions (cf. Ficken et al., 1998), including identifying the timing of fen-bog transitions in peat cores.

Conclusions

In this study we investigated whether biomarkers can be applied to distinguish fen and bog environments, and if plant-specific biomarkers can be identified from fen peat. Not surprisingly, the palaeobotanical analyses were able to clearly separate dry bog hummocks, moist lawns and wet fen habitats apart. With the biomarkers more robust conclusions could be drawn only when the biomarkers were combined with the macrofossil data, after which a similar kind of sub-division of peatland habitats was achieved as yielded by palaeobotanical analyses. In agreement with our previous study of fen plants, we confirm that using biomarker data from highly humified fen peat layers to achieve species level information of past plant assemblages is very challenging. Although we previously showed that certain sterols could be used as indicators for some plant groups (e.g. *Sphagnum* mosses or sedge roots), these signals were not translated into the highly humified peat. However, we were able to separate bog and fen habitats apart by the changes in *n*-alkane concentrations and the *n*-alkane ratios along the cores. Moreover, the transition zone between fen and bog habitats was characterized by high concentrations of sterols and triterpenoids originating from vascular plants. This proxy result seems to be applicable when reconstructing dominating plant groups during the highly humified peat phases, and may potentially also be used as a degradation measure as related to past changes in the water table level, and the following increase in level of decay as indicated here by the 5α(H)-stanols/Δ^5-sterol ratio, CPI-value, C/N ratio and high UOM.

Acknowledgements

We thank J. Menegazzo and M. West for help in the laboratory. We thank the reviewers for providing constructive suggestions for improving the paper. Funding from the Academy of Finland (codes 131409, 218101 and 201321) and the INTIMATE program via a COST STMS grant are acknowledged.

References

Andersson R (2012) Lipid biomarkers and other geochemical indicators in paleoenvironmental studies of two Arctic systems, a Russian permafrost peatland and marine sediments from Lomonosov Ridge. Doctoral thesis in Geochemistry, Stockholm University, Sweden.

Andersson, RA and Meyers PA (2012) Effect of climate change on delivery and degradation of lipid biomarkers in a Holocene peat sequence in the eastern European Russian arctic. *Organic Geochemistry* 53: 63-72.

Andersson RA, Kuhry P, Meyers P, Zebühr Y, Crill P and Mörth M (2011) Impacts of paleohydrological changes on n-alkane biomarker compositions of a holocene peat sequence in the eastern european russian arctic. *Organic Geochemistry* 42: 1065-1075.

Avsejs, LA, Nott CJ, Xie S, Maddy D, Chambers FM and Evershed RP (2002) 5-*n*-Alkylresorcinols as biomarkers of sedges in an ombrotrophic peat section. *Organic Geochemistry* 33: 861-867.

Baas M, Pancost R, Van Geel B and Sinninghe Damsté JS (2000) A comparative study of lipids in Sphagnum species. *Organic Geochemistry* 31: 535-541.

Barber K, Dumayne-Peaty L, Hughes P, Mauquoy D and Scaife R (1998). Replicability and variability of the recent macrofossil and proxy-climate record from raised bogs: Field stratigraphy and macrofossil data from Bolton fell moss and Walton moss, Cumbria, England. *Journal of Quarternary Science* 13: 515-528.

Bertrand O, Mansuy-Huault L, Montargès-Pelletier E, Losson B, Argant J, Ruffaldi P, Etienne D, Garnier E, Dezileau L, Faure P and Michels R (2012) Molecular evidence for recent land use change from a swampy environment to a pond (Lorraine, France). *Organic Geochemistry* 50:1-10.

Bingham EM, McClymont EL, Väliranta M, Mauquoy D, Roberts Z, Chambers FM, et al. (2010) Conservative composition of n-alkane biomarkers in Sphagnum species: Implications for palaeoclimate reconstruction in ombrotrophic peat bogs. *Organic Geochemistry* 41: 214-220.

Bush R T and McInerney F A (2013) Leaf wax n-alkane distributions in and across modern plants: Implications for paleoecology and chemotaxonomy. *Geochimica Et Cosmochimica Acta* 117: 161-179.

Corrigan, D., Kloos, C., O'Connor, C.S., Timoney, R.F. (1973). Alkanes from four species of Sphagnum moss. *Phytochemistry* 12, 213–214.

Dembitsky, V.M. (1993). Lipids of bryophytes. *Progress in Lipid Research* 32, 281–356.

Dudová L, Hájková P, Buchtová H and Opravilová V (2013) Formation, succession and landscape history of Central-European summit raised bogs: A multiproxy study from the Hrubý Jeseník mountains. *Holocene* 23:230-42.

Ficken KJ, Barber KE and Eglinton G (1998) Lipid biomarker, δ 13C and plant macrofossil stratigraphy of a Scottish montane peat bog over the last two millennia. *Organic Geochemistry* 28: 217-237.

Ficken, K.J., Li, B., Swain, D.L., Eglinton, G. (2000(. An n-alkane proxy for the sedimentary input of submerged/floating freshwater aquatic macrophytes. *Organic Geochemistry* 31, 745–749

Frolking S., Roulet N.T., Tuittila E-S., Bubier, J.L, Quillet, A, Talbot, J. Richard P.J.H. 2010. A new model of Holocene peatland net primary production, decomposition, water balance, and peat accumulation. *Earth System Dynamics* 1:1-21. doi:10.5194/esd-1-1-2010

Goad LJ and Akihisa T (1997) Analysis of sterols. Blackie Academic and Professional, Blackie Academic & Professional, London.

Hill MO and Šmilauer P (2005) WinTWINS version 2.3. Availeble at http://planet.uwc.ac.za/nisl/computing/Twinspan/userguide_twinspan.pdf (accessed 12 September 2013).

Huang X, Wang C, Zhang J, Wiesenberg GLB, Zhang Z and Xie S (2011) Comparison of free lipid compositions between roots and leaves of plants in the Dajiuhu Peatland, Central China. *Geochemical Journal* 45: 365-373.

Hughes, P.D.M. (2000) A reappraisal of the mechanisms leading to ombrotrophy in British raised mires. *Ecology Letters* 3 (1): 7-9.

Hughes, P.D.M. and Barber, K.E. (2003) Mire development across the fen-bog transition on the Teifi floodplain at Tregaron Bog, Ceredigion, Wales, and a comparison with 13 other raised bogs. *Journal of Ecology* 91 (2): 253-264.

Jia G, Dungait JAJ, Bingham EM, Valiranta M, Korhola A and Evershed RP (2008) Neutral monosaccharides as biomarker proxies for bog-forming plants for application to palaeovegetation reconstruction in ombrotrophic peat deposits. *Organic Geochemistry* 39: 1790-1799.

Killops SD and Frewin NL (1994) Triterpenoid diagenesis and cuticular preservation. *Organic Geochemistry* 21: 1193-1209.

Kuhry P and Vitt DH (1996) Fossil carbon/nitrogen ratios as a measure of peat decomposition. *Ecology* 77: 271-275.

Laine AM, Byrne KA, Kiely G and Tuittila E- (2007) Patterns in vegetation and CO_2 dynamics along a water level gradient in a lowland blanket bog. *Ecosystems* 10: 890-905.

Laine, A. Juurola, E., Hajek, T., Tuittila, E-S. 2011*Sphagnum* growth and ecophysiology during mire succession. *Oecologia* 167: 1115-1125. DOI: 10.1007/s00442-011-2039-4

Larmola T., Leppänen, S. Tuittila E-S., Aarva M., Merilä P., Fritze H. and Tiirola, M. Methanotrophy induces nitrogen fixation during peatland development. Accepted to be published in *Proceedings of the National Academy of Sciences* in November 2013.

Lehtonen K and Ketola M (1993) Solvent-extractable lipids of Sphagnum, Carex, Bryales and Carex-Bryales peats: content and compositional features vs peat humification. *Organic Geochemistry* 20: 363-380.

Leppälä M, Laine AM, Seväkivi M- and Tuittila E- (2011) Differences in CO2 dynamics between successional mire plant communities during wet and dry summers. *Journal of Vegetation Science* 22: 357-366.

Leppälä, M., Oksanen, J. and Tuittila E-S. 2011. Methane flux dynamics during mire succession. *Oecologia* 165:489–499. DOI 10.1007/s00442-010-1754-6

Levy PE, Burden A, Cooper MDA, Dinsmore KJ, Drewer J, Evans C, et al. (2012) Methane emissions from soils: Synthesis and analysis of a large UK data set. *Global Change Biology* 18: 1657-1669.

Loisel J and Yu Z (2013) Recent acceleration of carbon accumulation in a boreal peatland, south central Alaska. *Journal of Geophysical Research G: Biogeosciences*. 118:41-53.

López-Días V, Borrego T, Blanco CG, Arboleya M, López-Sáez JA and López-Merino L (2010) Biomarkers in a peat deposit in Northern Spain (Huelga de Bayas, Asturias) as proxy for climate variation. *Journal of Chromatography A* 1217: 3538-3546.

Matthews E (2000). Wetlands. In: Khalil MAK (eds) *Atmospheric methane. Its role in the Global Environment.* Berlin: Springer Verlag, pp. 202-233.

Mauquoy D, Engelkes T, Groot MHM, Markesteijn F, Oudejans MG, Van Der Plicht J, et al. (2002) High-resolution records of late-Holocene climate change and carbon accumulation in two north-west European ombrotrophic peat bogs. *Palaeogeography, Palaeoclimatology, Palaeoecology* 186: 275-310.

McClymont EL, Mauquoy D, Yeloff D, Broekens P, Van Geel B, Charman DJ, et al. (2008) The disappearance of Sphagnum imbricatum from Butterburn Flow, UK. *Holocene* 18: 991-1002.

McClymont, E.L., Pancost, R.D., Bingham, E.M., Childs, E.V., Charman, D., Blundell, A., Chambers, F.M. and Evershed, R.P. (under review, 2013) Application of the stanol:Δ^5sterol ratio as a proxy for palaeoredox conditions in mires. Submitted to *Organic Geochemistry*.

Mauquoy, D., Van Geel, B., Blaauw, M. and Van der Plicht, J. (2002). Evidence from northwest European bogs shows 'Little Ice Age' climatic changes driven by variations in solar activity. *Holocene* 12 : 1-6.

Meyers PA (2003) Applications of organic geochemistry to paleolimnological reconstructions: A summary of examples from the Laurentian Great Lakes. *Organic Geochemistry* 34: 261-289.

Moore TR, Bubier JL and Bledzki L (2007) Litter decomposition in temperate peatland ecosystems: The effect of substrate and site. *Ecosystems* 10: 949-963.

Nichols JE, Booth RK, Jackson ST, Pendall EG and Huang Y (2006) Paleohydrologic reconstruction based on n-alkane distributions in ombrotrophic peat. *Organic Geochemistry* 37: 1505-1513.

Nissinen, R. and Sewón, P. (1994). Hydrocarbons of Polytrichum commune. *Phytochemistry* 37, 179–182.

Nott CJ, Xie S, Avsejs LA, Maddy D, Chambers FM, and Evershed RP (2000) *n*-Alkane distributions in ombrotrophic mires as indicators of vegetation change related to climatic variation. *Organic Geochemistry* 31: 231-235.

Ortiz J.E., Gallego J.L.R., Torres T., Díaz-Bautista A. Sierra C. 2010. Palaeoenvironmental reconstruction of Northern Spain during the last 8000 cal yr BP based on the biomarker content of the Roñanzas peat bog (Asturias). Organic Geochemistry 41: 454-466.

Ortiz JE, Díaz-Bautista A, Aldasoro JJ, Torres T, Gallego JLR, Moreno L, et al. (2011) *n*-Alkan-2-ones in peat-forming plants from the Roñanzas ombrotrophic bog (Asturias, northern Spain). *Organic Geochemistry* 42: 586-592.

Pancost RD, Baas M, Van Geel B and Sinninghe Damsté JS (2002) Biomarkers as proxies for plant inputs to peats: An example from a sub-boreal ombrotrophic bog. *Organic Geochemistry* 33: 675-690.

Riutta T, Laine J, Aurela M, Rinne J, Vesala T, Laurila T, et al. (2007) Spatial variation in plant community functions regulates carbon gas dynamics in a boreal fen ecosystem. *Tellus, Series B: Chemical and Physical Meteorology* 59): 838-852.

Ronkainen T, McClymont EL, Väliranta M, Tuittila E-T (2013) The *n*-alkane and sterol composition of living fen plants as a potential tool for palaeoecological studies. *Organic Geochemistry* 59: 1-9.

Rydin H, Jeglum JK and Hooijer A (2006) *The Biology of Peatlands.* Oxford: Oxford University Press.

Salasoo, I. (1987). Epicuticular wax alkanes of some heath plants in central Alaska. *Biochemical Systematics and Ecology* 15, 105–107.

Sachse, D., Radke, J., Gleixner, G. (2006). DD values of individual n-alkanes from terrestrial plants along a climatic gradient – implications for the sedimentary biomarker record. *Organic Geochemistry* 37, 469–483.

Speranza, A., Van Der Plicht, J.and Van Geel, B. (2000) Improving the time control of the Subboreal/Subatlantic transition in a Czech peat sequence by 14C wiggle-matching. *Quaternary Science Reviews* 19: 1589-1604.

ter Braak CJFP and Šmilauer P (2002) CANOCO reference manual and CanoDraw for Windows user's guide: Software for canonical community ordination (version 4.5). NY, Ithaca: Microcomputer Power.

Tuittila E-S, Väliranta M, Laine A and Korhola A (2007) Controls of mire vegetation succession in a southern boreal bog. *Journal of Vegetation Science* 18: 891-902.

Tuittila E-S, Juutinen S, Frolking S, Väliranta, M, Miettinen A, Laine A, Quillet A and Merilä P (2013) Wetland chronosequence as a model of peatland development: Vegetation succession, peat and carbon accumulation. *Holocene* 23: 25-35.

Turunen J, Tomppo E, Tolonen K, et al. (2002) Estimating carbon accumulation rates of undrained mires in Finland: application to boreal and subarctic regions. The Holocene 12: 69-80.

Wheeler BD and Proctor MCF (2000) Ecological gradients, subdivisions and terminology of north-west European mires. *Journal of Ecology* 88: 187-203.

Vonk JE and Gustafsson O (2009) Calibrating n-alkane Sphagnum proxies in sub-Arctic Scandinavia. *Organic Geochemistry* 40: 1085-1090.

Väliranta M, Korhola A, Seppä H, Tuittila E-, Sarmaja-Korjonen K, Laine J, et al. (2007) High-resolution reconstruction of wetness dynamics in a southern boreal raised bog, Finland, during the late Holocene: A quantitative approach. *Holocene* 17: 1093-1107.

Yu Z, Loisel J, Turetsky MR, Cai S, Zhao Y, Frolking S, et al. (2013) Evidence for elevated emissions from high-latitude wetlands contributing to high atmospheric CH4 concentration in the early Holocene. *Global Biogeochem Cycles* 27:131-40.

Yu Z, Loisel J, Brosseau DP, Beilman,DW and Hunt SJ (2010) Global peatland dynamics since the Last Glacial Maximum. *Geophysical Research Letters* 37: L13402.

Xie S, Nott CJ, Avsejs LA, Volders F, Maddy D, Chambers FM, et al. (2000) Palaeoclimate records in compound-specific δD values of a lipid biomarker in ombrotrophic peat. *Organic Geochemistry* 31: 1053-1057.

Xie S, Nott CJ, Avsejs LA, Maddy D, Chambers FM and Evershed RP (2004) Molecular and isotopic stratigraphy in an ombrotrophic mire for paleoclimate reconstruction. *Geochimica et Cosmochimica Acta* 68: 2849-2862.

Zech, M., Andreev, A., Zech, R., Müller, S., Hambach, U., Frechen, M., Zech, W. (2010). Quaternary vegetation changes derived from a loess-like permafrost palaeosol sequence in northeast Siberia using alkane biomarker and pollen analyses. *Boreas* 39, 540–550.

Økland RH, Okland T and Rydgren K (2001) A Scandinavian perspective on ecological gradients in north-west European mires: Reply to Wheeler and Proctor. *Journal of Ecology 89*: 481-486.

Table caption:

Table 1. Macrofossil and biomarker communities in peat cores SJ5 and SJ6 derived from TWINSPAN (n=72, macrofossils and biomarkers in the data). Five cut levels and two divisions were used.

Supplementary data table 1. File includes published distributions of biomarkers in plants mentioned in the study.

Supplementary data table 2. File includes all the biomarker data used in the analysis.

Fig.1. Location of the study site. Samples were collected from two closely situated peatlands from the Siikajoki commune ((64°45´N, 24°42´E), Finland, Northern-Europe.
86x93mm (600 x 600 DPI)

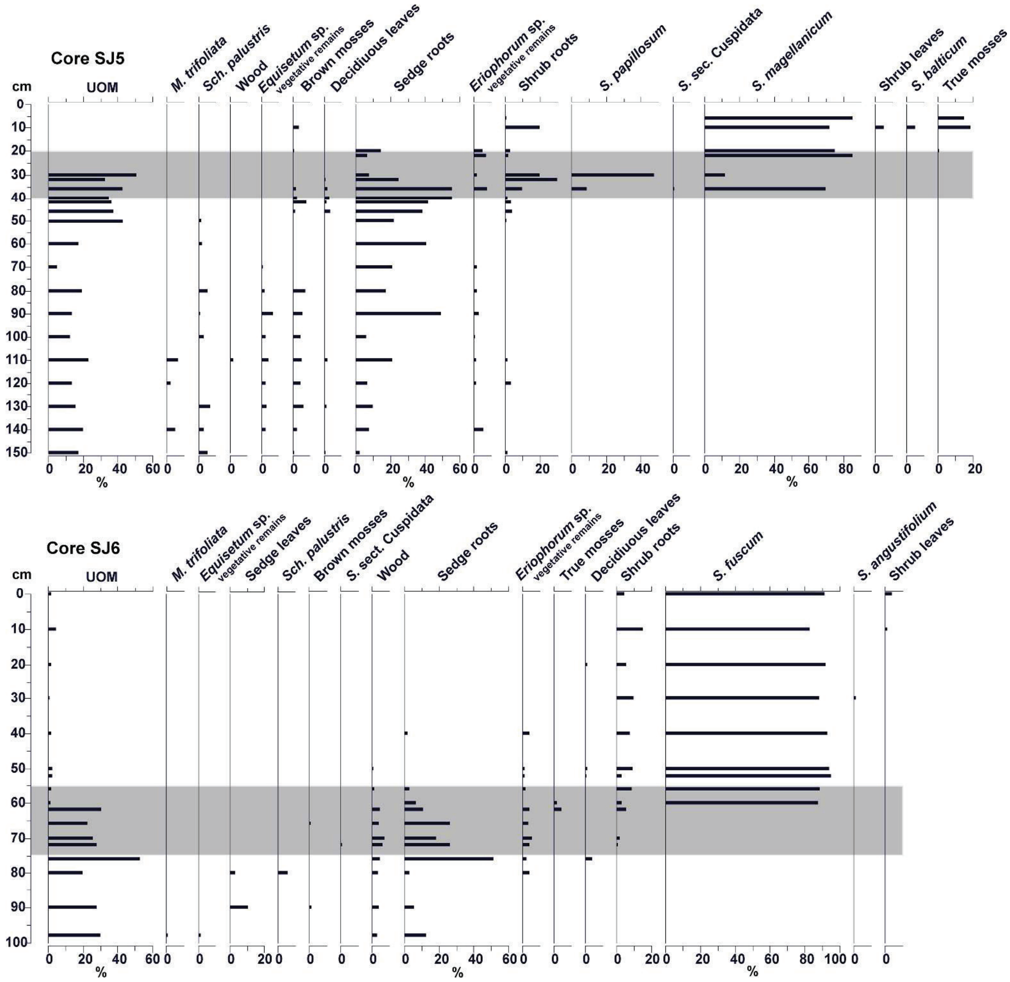

Fig. 2. Plant macrofossil records of cores SJ5 and SJ6. Macrofossil abundances are expressed as proportions (%). The fen-bog transition zone is marked with gray bar.
200x195mm (600 x 600 DPI)

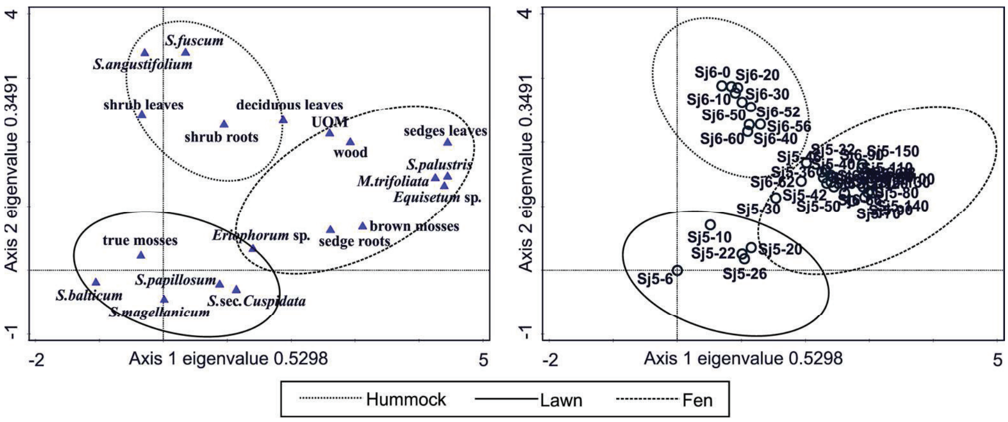

Fig. 3. DCA results of the macrofossil data of cores SJ5 and SJ6. The first axis explains 28 % (eigenvalue 0.5298) and the second axis 18 % (eigenvalue 0.3491) of the variation in the macrofossil data. Species representing hummock, lawn and fen habitats are circulated.
81x33mm (600 x 600 DPI)

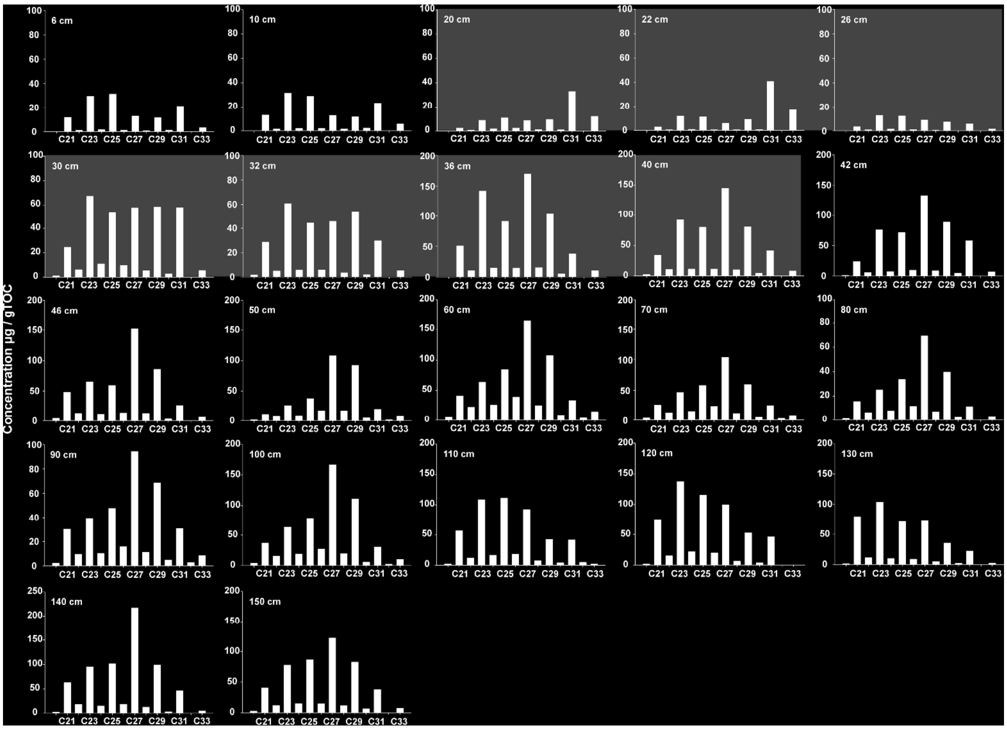

Fig. 4a. *n*-alkane concentrations (µg/gTOC) of core SJ6 by depth. The fen-bog transition zone is marked with gray.
191x137mm (600 x 600 DPI)

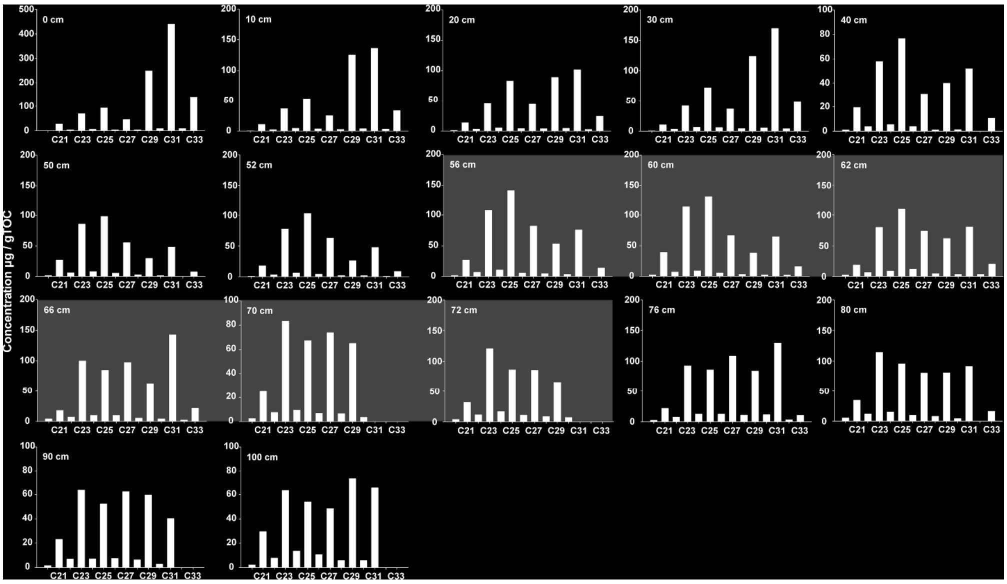

Fig. 4b. *n*-alkane concentrations (μg/gTOC) of core SJ6 by depth. The fen-bog transition zone is marked with gray.
168x96mm (600 x 600 DPI)

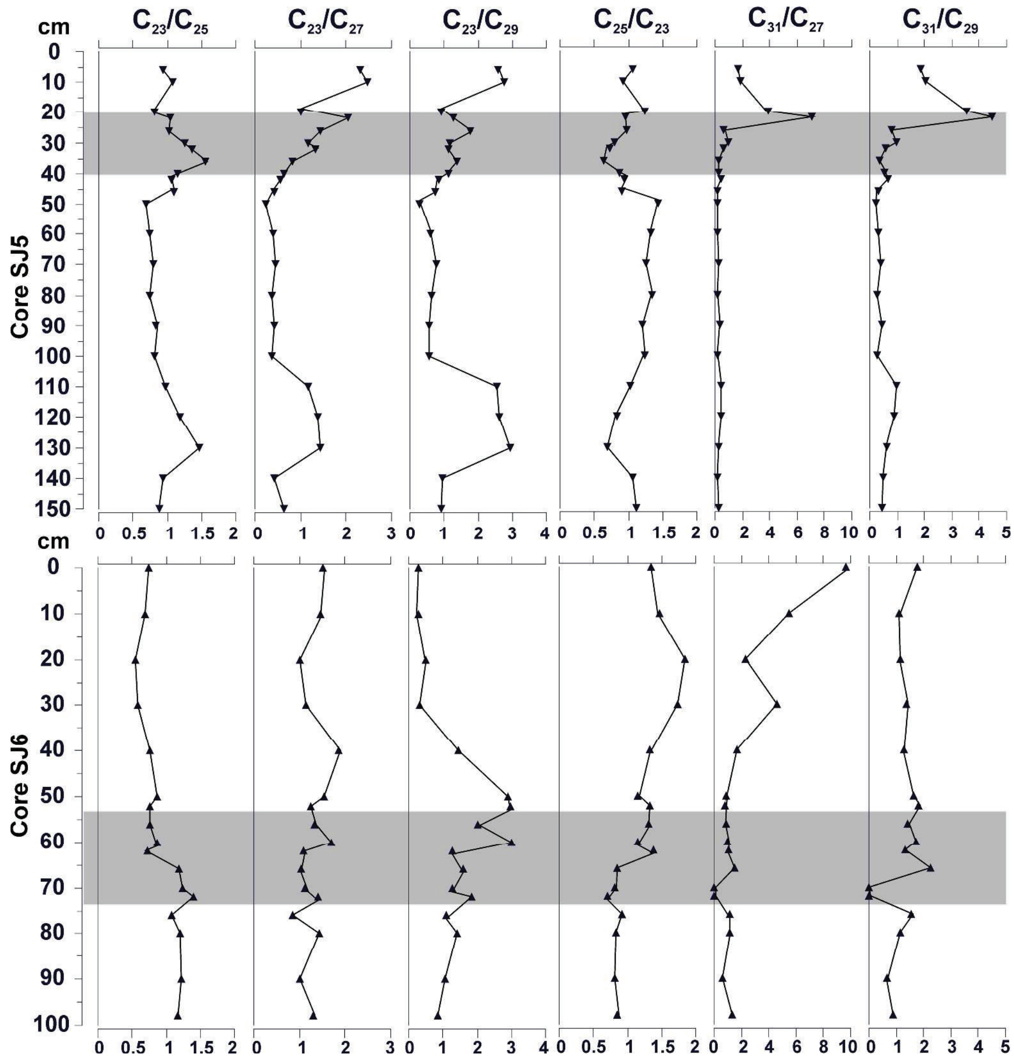

Fig. 5. *n*-alkane ratios of cores SJ5 and SJ6. The fen-bog transition zone is marked with gray bar.
188x196mm (600 x 600 DPI)

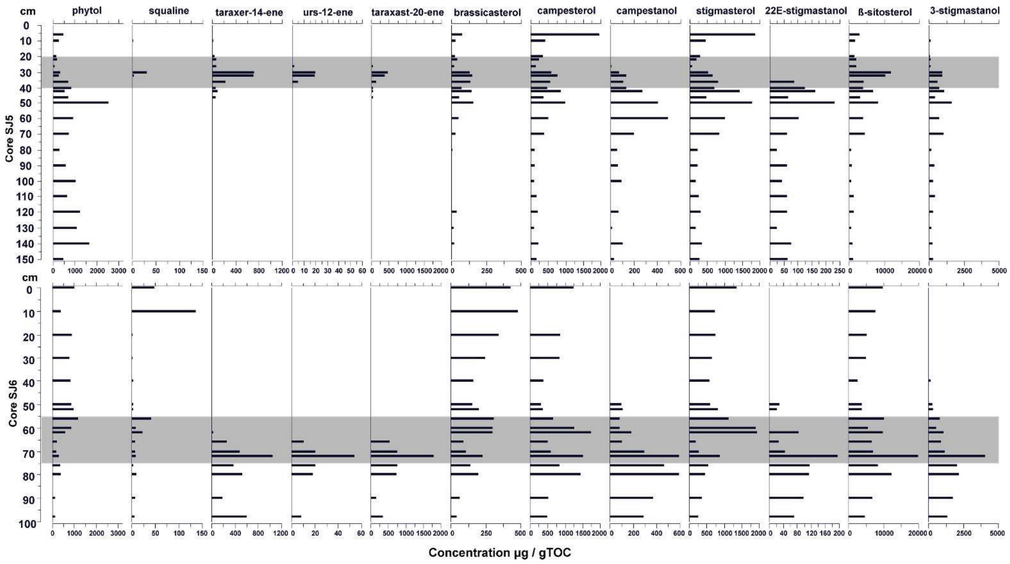

Fig. 6. Concentrations (µg/gTOC) of triterpenoids, Δ^5-sterols and 5α(H)-stanols in cores SJ5 and SJ6. The fen-bog transition zone is marked with gray bar.
161x89mm (600 x 600 DPI)

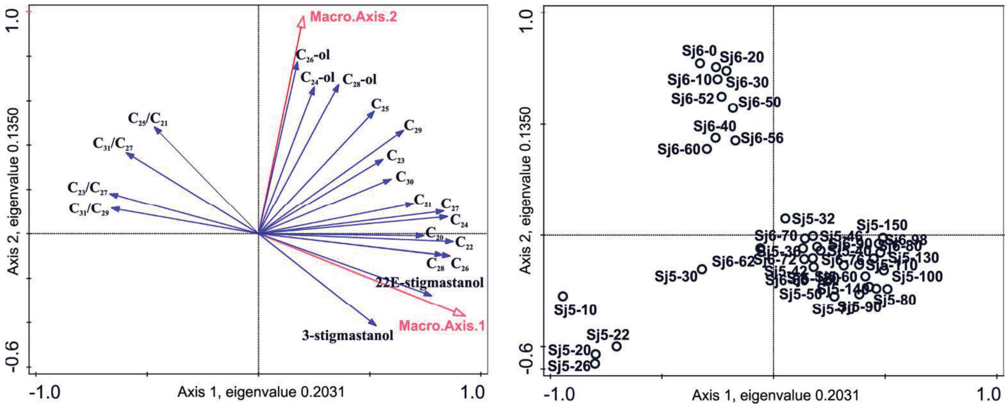

Fig. 7. RDA of biomarker data of cores SJ5 and SJ6, case scores Macro.axis.1 and Macro.axis.2 from macrofossil DCA as explanatory variables. The first axis explains 20 % (eigenvalue 0.2031) and the second axis 13 % (eigenvalue 0.1350) of the variation in the biomarker data (pseudo F = 9.2 and *p*-value = 0.002). In the figure 20 (out of 54) best fitted biomarkers are presented.
76x30mm (600 x 600 DPI)

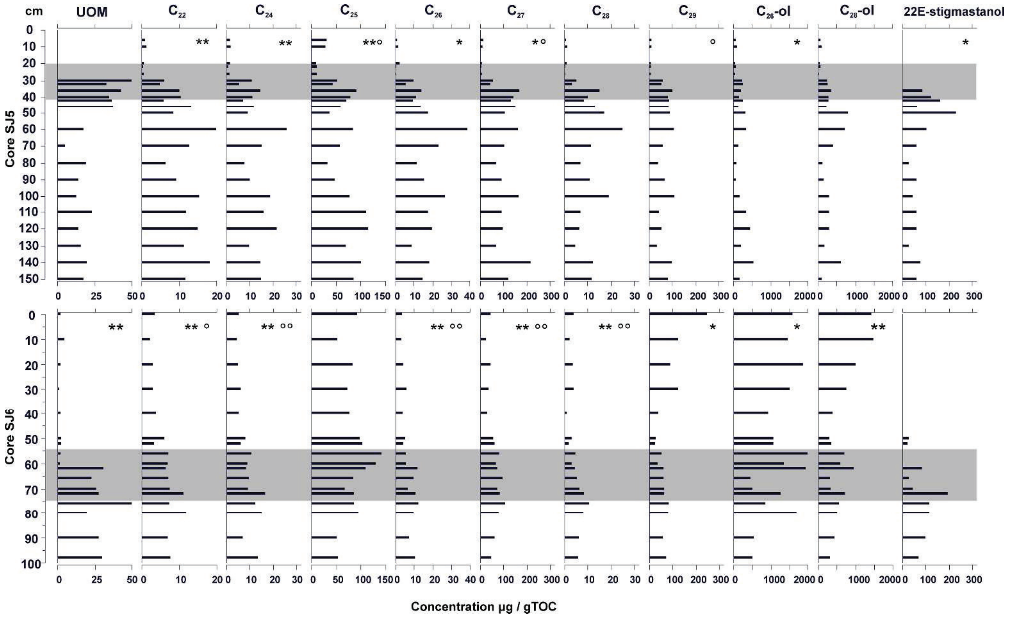

Fig. 8. Concentrations (µg/gTOC) of 10 best fitted biomarkers from biomarker RDA in cores SJ5 and SJ6. Compounds correlating with depth (sig. 0.05=*, sig. 0.01=**) and UOM (sig. 0.05=°, sig 0.01=°°) are marked. The fen-bog transition zone in both cores is marked with gray.
173x105mm (600 x 600 DPI)

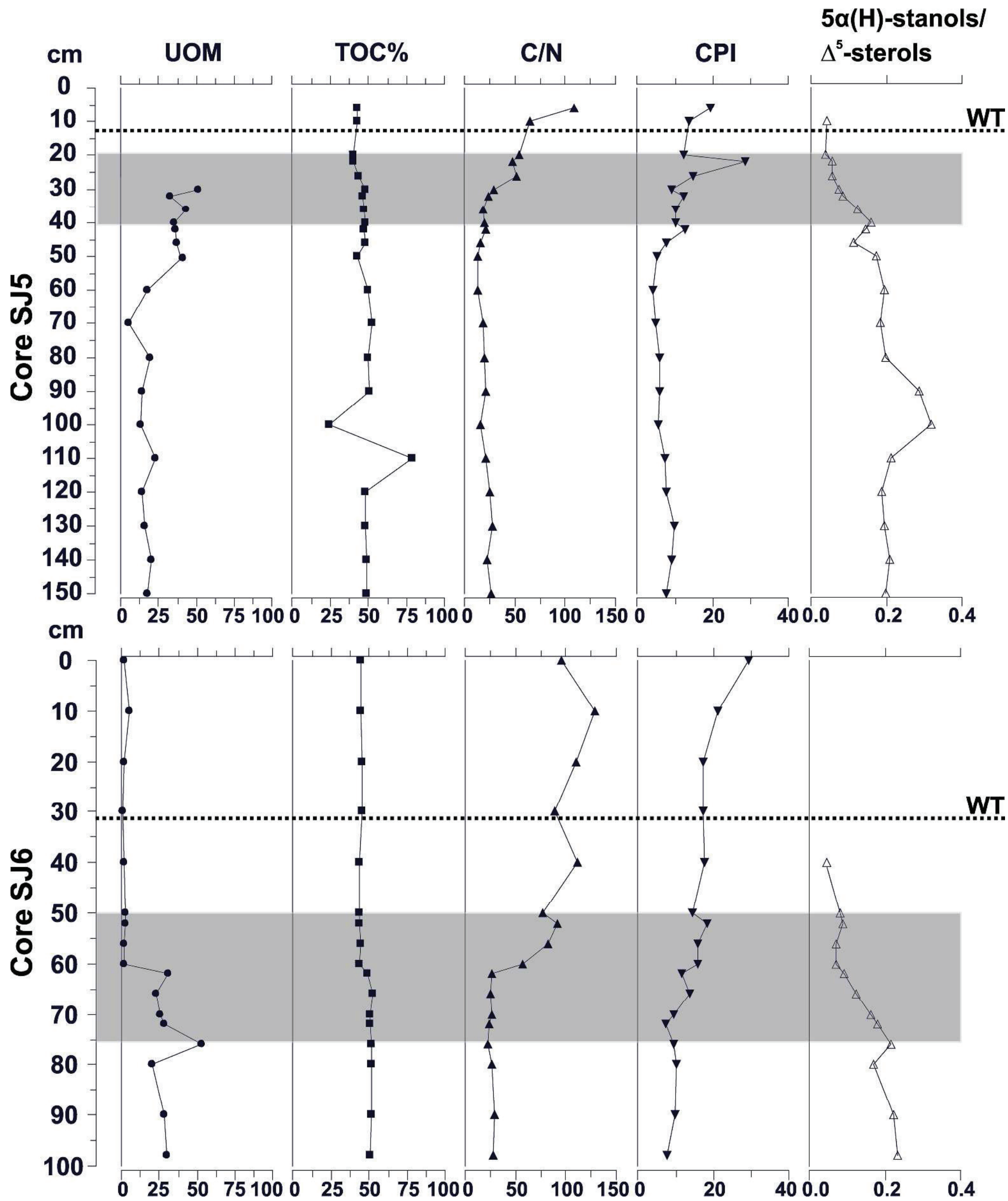

Fig. 9. Degradation measures in cores SJ5 and SJ6. UOM and TOC are presented as %, C/N ratio, CPI-value (= $CPI_{alk}=((C_{21}-C_{31})+(C_{23}-C_{33})odd/2*(C_{22}-C_{32})even)$ according to Andersson and Mayers, 2012) and the 5α(H)-stanols/Δ^5-sterol ratio (=(campestanol+22E-stigmastanol+3-stigmastanol)/(campesterol+campestanol+stigmasterol+ 22E-stigmastanol+β-sitosterol+3-stigmastanol)) according to McClymony et al., 2013) The fen-bog transition zone is marked with gray bar and water table level (WT) with dashed line.
169x201mm (600 x 600 DPI)

First division	Second division
Hummock-fen *n* = 33 *S. fuscum, Equisetum* sp., *Sch. palustris* , wood, deciduous leaves, UOM campestanol, C_{20}-ol 22E-stigmastanol C_{27}, C_{20}, C_{32}	**Hummock *n* = 9** *S. fuscum,* shrub leaves C_{27}- ol, C_{34}, squaline **Fen *n* = 24** brown mosses, sedge roots *Equisetum* sp., *Sch. palustris* *M. trifoliata* , campestanol, 22E-stigmastanol, urs-20-ene
Lawn *n* = 6 *S. magellanicum, S. papillosum* *S. balticum* , *S.* sect. Cuspidata true-mosses, urs-20-ene	

Table 1

Plant	Major homologue associated to plant	Studied plant species
S. fuscum	*n*-C_{25} [c, b, i, k, m]	
S. angustifolium	*n*-C_{23} [l]	
S. magellanicum	*n*-C_{25} [l]	
S. papillosum	*n*-C_{23} [l], *n*-C_{25} [l]	
S. balticum	*n*-C_{23} [l, m]	
S. sec.*Cuspidata*	*n*-C_{23} [m, o]	*S. balticum* [m], *S. lindbergii* [m], S. angustifolium [l], *S. cuspidatum* [l], *S. maju* s [l], *S. tenellum* [l], *S. riparium* [o]
True mosses	*n*-C_{27} [h], *n*-C_{31} [e, m]	*Polytrichum* sp. [e, h], *Dicranum elongatum* [m]
Brown mosses	*n*-C_{25} [o], *n*-C_{27} [o]	*Warnstorfia exannulata* [o]
M. trifoliata leaves	*n*-C_{29} [o]	
M. trifoliata roots	*n*-C_{21} [o], *n*-C_{23} [o]	
Equisetum sp.	no reference	
S. palustris	no reference	
Eriophorum sp. leaves	*n*-C_{27} [o, q], *n*-C_{29} [m]	
Eriophorum sp roots	*n*-C_{27} [o, m,]	
Sedge leaves	*n*-C_{27} [b, m], *n*-C_{29} [f, o] or *n*-C_{31} [f, o]	*Carex* sp. [b, f, m, o]
Sedge roots	*n*-C_{21} [o], *n*-C_{23} [m, o], *n*-C_{27} [o],	
Shrub leafs	*n*-C_{27} [d, j, q], *n*-C_{29} [b, q], *n*-C_{31} [a, q]	*Ledum* sp.[a, m], *V. vitis-idaea* [b], *B. nana* [d ,j, m], *E. nigrum* [m], *V. uliginossum* [m], several species [q]
Shrub root	*n*-C_{27} [m], *n*-C_{29} [m], *n*-C_{31} [n]	*Eriacaceae* [n], *Betula nana* [n, m], *L. palustris* [m], *E. nigrum* [m], *V. uliginossum* [m]
Wood	*n*-C_{27} [m]	*Betula* (tree)[m]
Deciduous leaves	*n*-C_{27} [m, q], *n*-C_{29} [m, q]	*Betula* (tree)[m], several species [q]
Conifer needles	*n*-C_{27} [q], *n*-C_{29} [q], *n*-C_{31} [q]	several species [q]

[a] (Salasoo, 1987); [b] (Ficken et al., 1998); [c] (Corrigan et al., 1973); [d] (Sachse et al., 2006); [e] (Nott et al., 2000); [f] (Ficken et al., 2000); [g] (Baas et al., 2000); [h] (Nissinen and Sewón, 1994); [i] (Vonk and Gustafsson, 2009);[j] (Zech et al., 2010); [k] (Dembitsky, 1993); [l] (Bingham et al., 2010); [m] (Ronkainen et al. submitted); [n] (Andersson et al., 2011); [o] (Ronkainen et al. 2013); [q] (Tarasov et al., 2013)

n- alkanes

Sample	C20	C21	C22	C23	C24	C25	C26	C27	C28	C29	C30	C31	C32	C33	C34	C35
SJ5: 6	-	11.5	1.1	29.6	1.7	31.5	1.2	12.8	0.8	11.4	1.2	21.4	-	3.3	-	-
SJ5: 10	-	12.9	1.4	31.5	1.9	29.0	1.9	12.7	1.5	11.4	2.2	23.1	-	5.5	-	-
SJ5: 20	-	2.3	0.7	8.7	1.7	10.7	2.3	8.6	1.0	9.3	0.8	33.0	-	11.9	-	-
SJ5: 22	-	3.0	0.5	11.8	0.9	11.3	0.5	5.8	0.5	9.2	0.7	41.0	-	17.1	-	-
SJ5: 26	-	3.2	0.8	12.6	1.3	12.2	0.8	8.8	0.6	7.1	-	5.8	-	1.5	-	-
SJ5: 30	1.2	24.7	6.2	67.2	11.0	53.2	9.8	57.6	5.4	58.2	2.8	57.8	-	5.7	-	-
SJ5: 32	1.7	28.6	4.9	60.8	5.6	44.3	5.7	45.5	3.4	53.2	1.8	29.6	-	5.2	-	-
SJ5: 36	-	50.8	10.3	142.0	14.7	91.0	14.2	170.2	15.2	103.3	5.0	37.7	-	10.3	-	-
SJ5: 40	2.3	33.9	10.6	92.2	11.3	80.0	11.3	145.2	10.1	80.8	4.5	41.4	-	8.1	-	0.7
SJ5: 42	1.2	24.1	6.0	76.0	7.4	71.7	9.5	133.1	8.6	88.7	4.9	58.0	-	7.1	-	-
SJ5: 46	4.2	48.0	13.3	64.9	12.0	59.1	13.8	152.1	13.3	85.7	3.3	26.4	-	6.7	-	-
SJ5: 50	1.5	11.6	8.6	26.1	9.3	37.4	17.6	108.0	17.3	92.0	4.8	20.0	1.5	9.1	-	1.4
SJ5: 60	4.9	41.0	22.3	63.5	26.1	84.4	39.0	164.1	25.2	107.1	9.2	33.4	3.9	14.9	-	1.3
SJ5: 70	3.2	25.7	12.9	46.2	15.2	57.9	23.4	103.9	11.6	59.1	4.5	24.8	2.7	8.4	-	-
SJ5: 80	1.2	15.6	6.5	25.1	7.9	33.8	11.7	69.5	7.1	39.8	2.1	11.3	-	3.2	-	-
SJ5: 90	2.2	30.0	9.3	39.4	10.2	47.7	15.7	94.3	11.0	68.6	4.6	30.5	2.8	8.3	1.0	1.6
SJ5: 100	3.7	37.0	15.5	63.2	19.0	78.4	27.1	166.7	19.4	110.8	5.6	30.5	2.3	10.3	-	1.9
SJ5: 110	2.1	56.6	11.9	108.6	16.3	111.4	17.9	92.5	7.1	42.4	3.9	41.7	4.8	1.9	-	-
SJ5: 120	1.6	74.7	15.0	137.2	21.9	115.1	20.0	99.5	6.5	52.7	3.6	46.2	-	-	-	-
SJ5: 130	1.5	79.8	11.4	103.5	10.0	70.6	8.9	72.0	4.9	35.3	1.9	22.1	-	2.4	-	-
SJ5: 140	2.0	62.5	18.2	94.6	14.8	101.0	18.5	217.3	12.4	98.6	2.9	46.2	-	4.4	-	-
SJ5: 150	2.6	40.6	11.8	77.6	15.0	86.9	14.7	122.1	11.8	82.8	6.6	37.7	-	7.4	-	-

Sample	C20	C21	C22	C23	C24	C25	C26	C27	C28	C29	C30	C31	C32	C33	C34	C35
SJ6: 0	0.6	27.8	3.5	69.4	5.3	93.4	3.7	45.8	4.1	248.6	8.5	439.9	8.8	140.2	0.8	-
SJ6: 10	0.3	10.8	2.3	36.4	4.5	53.3	3.3	24.9	2.4	125.5	3.6	136.2	3.0	33.1	-	-
SJ6: 20	1.0	13.5	2.9	45.0	5.2	83.0	4.1	44.1	3.6	89.3	4.4	101.8	2.4	24.4	0.6	-
SJ6: 30	0.5	10.3	2.9	41.7	6.2	72.4	5.8	36.5	4.0	124.0	5.3	169.7	3.9	48.0	-	-
SJ6: 40	1.1	19.5	3.9	57.9	5.5	76.7	3.9	31.1	1.1	40.1	1.4	51.9	-	10.6	-	-
SJ6: 50	1.8	26.8	6.1	85.7	8.1	98.2	5.3	55.4	3.0	29.6	1.6	48.2	-	7.4	-	-
SJ6: 52	0.7	17.8	3.3	77.6	6.2	103.0	4.2	62.7	2.1	26.1	1.6	47.6	0.9	8.6	-	-
SJ6: 56	1.8	26.8	7.1	108.0	10.7	141.5	5.7	82.1	4.7	53.2	3.2	75.7	-	13.7	-	-
SJ6: 60	2.4	39.1	7.0	113.9	9.0	130.4	5.5	66.7	3.0	38.0	2.4	64.8	1.9	15.9	-	-
SJ6: 62	2.4	18.8	6.4	79.8	8.5	109.8	11.9	74.0	4.5	61.9	3.2	80.8	3.3	20.1	-	-
SJ6: 66	4.2	17.8	7.2	100.1	9.6	84.9	9.7	97.2	5.4	63.1	4.1	142.5	2.1	21.3	-	-
SJ6: 70	2.5	25.1	7.6	83.2	9.4	67.2	6.8	73.9	6.6	65.0	3.5	-	-	-	-	-
SJ6: 72	3.6	31.9	11.2	120.5	16.6	85.8	10.9	85.3	8.6	65.5	6.9	-	-	-	-	-
SJ6: 76	2.4	21.6	7.4	92.5	12.4	85.8	12.4	108.5	10.7	83.9	11.3	129.4	3.2	10.4	-	-
SJ6: 80	5.2	34.6	11.9	114.3	15.2	95.4	9.8	80.3	8.1	80.8	4.4	91.4	-	16.5	-	-
SJ6: 90	1.5	23.2	7.0	63.7	7.2	52.4	7.5	62.4	6.3	59.7	2.9	40.3	-	-	-	-
SJ6: 98	2.1	29.6	7.8	63.5	13.7	54.0	10.6	48.5	5.8	73.9	5.8	65.7	-	-	-	-

Concentrations are presented as µg gTOC

n- alkane ratios

Sample	C23/C25	C23/C27	C23/C29	C23/C31	C25/C29	C31/C27	C31/C29	C33/C31	C23/(C23+C29)
SJ5: 6	0.9	2.3	2.6	1.4	2.8	1.7	1.9	0.2	0.7
SJ5: 10	1.1	2.5	2.8	1.4	2.5	1.8	2.0	0.2	0.7
SJ5: 20	0.8	1.0	0.9	0.3	1.2	3.9	3.6	0.4	0.5
SJ5: 22	1.0	2.0	1.3	0.3	1.2	7.0	4.5	0.4	0.6
SJ5: 26	1.0	1.4	1.8	2.2	1.7	0.7	0.8	0.3	0.6
SJ5: 30	1.3	1.2	1.2	1.2	0.9	1.0	1.0	0.1	0.5
SJ5: 32	1.4	1.3	1.1	2.1	0.8	0.7	0.6	0.2	0.5
SJ5: 36	1.6	0.8	1.4	3.8	0.9	0.2	0.4	0.3	0.6
SJ5: 40	1.2	0.6	1.1	2.2	1.0	0.3	0.5	0.2	0.5
SJ5: 42	1.1	0.6	0.9	1.3	0.8	0.4	0.7	0.1	0.5
SJ5: 46	1.1	0.4	0.8	2.5	0.7	0.2	0.3	0.3	0.4
SJ5: 50	0.7	0.2	0.3	1.3	0.4	0.2	0.2	0.5	0.2
SJ5: 60	0.8	0.4	0.6	1.9	0.8	0.2	0.3	0.4	0.4
SJ5: 70	0.8	0.4	0.8	1.9	1.0	0.2	0.4	0.3	0.4
SJ5: 80	0.7	0.4	0.6	2.2	0.8	0.2	0.3	0.3	0.4
SJ5: 90	0.8	0.4	0.6	1.3	0.7	0.3	0.4	0.3	0.4
SJ5: 100	0.8	0.4	0.6	2.1	0.7	0.2	0.3	0.3	0.4
SJ5: 110	1.0	1.2	2.6	2.6	2.6	0.5	1.0	0.0	0.7
SJ5: 120	1.2	1.4	2.6	3.0	2.2	0.5	0.9	0.0	0.7
SJ5: 130	1.5	1.4	2.9	4.7	2.0	0.3	0.6	0.1	0.7
SJ5: 140	0.9	0.4	1.0	2.0	1.0	0.2	0.5	0.1	0.5
SJ5: 150	0.9	0.6	0.9	2.1	1.0	0.3	0.5	0.2	0.5

Sample	C23/C25	C23/C27	C23/C29	C23/C31	C25/C29	C31/C27	C31/C29	C33/C31	C23/(C23+C29)
SJ6: 0	0.7	1.5	0.3	0.2	0.4	9.6	1.8	0.3	0.2
SJ6: 10	0.7	1.5	0.3	0.3	0.4	5.5	1.1	0.2	0.2
SJ6: 20	0.5	1.0	0.5	0.4	0.9	2.3	1.1	0.2	0.3
SJ6: 30	0.6	1.1	0.3	0.2	0.6	4.6	1.4	0.3	0.3
SJ6: 40	0.8	1.9	1.4	1.1	1.9	1.7	1.3	0.2	0.6
SJ6: 50	0.9	1.5	2.9	1.8	3.3	0.9	1.6	0.2	0.7
SJ6: 52	0.8	1.2	3.0	1.6	3.9	0.8	1.8	0.2	0.7
SJ6: 56	0.8	1.3	2.0	1.4	2.7	0.9	1.4	0.2	0.7
SJ6: 60	0.9	1.7	3.0	1.8	3.4	1.0	1.7	0.2	0.7
SJ6: 62	0.7	1.1	1.3	1.0	1.8	1.1	1.3	0.2	0.6
SJ6: 66	1.2	1.0	1.6	0.7	1.3	1.5	2.3	0.1	0.6
SJ6: 70	1.2	1.1	1.3	-	1.0	0.0	0.0	-	0.6
SJ6: 72	1.4	1.4	1.8	-	1.3	0.0	0.0	-	0.6
SJ6: 76	1.1	0.9	1.1	0.7	1.0	1.2	1.5	0.1	0.5
SJ6: 80	1.2	1.4	1.4	1.3	1.2	1.1	1.1	0.2	0.6
SJ6: 90	1.2	1.0	1.1	1.6	0.9	0.6	0.7	0.0	0.5
SJ6: 98	1.2	1.3	0.9	1.0	0.7	1.4	0.9	0.0	0.5

n- alkane ratios

Sample	C25/(C25+C29)	C23/(C27+C31)	Paq	ACL C17-C35	Pwax	C23/C21	C21/C23	C25/C21	C25/C23
SJ5: 6	1.0	0.9	0.7	26.0	0.4	2.6	0.4	2.7	1.1
SJ5: 10	0.9	0.9	0.6	26.1	0.4	2.4	0.4	2.3	0.9
SJ5: 20	0.8	0.2	0.3	28.8	0.7	3.8	0.3	4.6	1.2
SJ5: 22	1.0	0.3	0.3	29.0	0.7	4.0	0.3	3.8	1.0
SJ5: 26	0.9	0.9	0.7	26.1	0.5	3.9	0.3	3.8	1.0
SJ5: 30	0.8	0.6	0.5	26.5	0.6	2.7	0.4	2.2	0.8
SJ5: 32	0.9	0.8	0.6	26.0	0.5	2.1	0.5	1.5	0.7
SJ5: 36	0.9	0.7	0.6	25.9	0.6	2.8	0.4	1.8	0.6
SJ5: 40	0.9	0.5	0.6	26.2	0.6	2.7	0.4	2.4	0.9
SJ5: 42	0.9	0.4	0.5	26.7	0.7	3.2	0.3	3.0	0.9
SJ5: 46	0.8	0.4	0.5	26.1	0.7	1.4	0.7	1.2	0.9
SJ5: 50	0.7	0.2	0.4	27.2	0.8	2.3	0.4	3.2	1.4
SJ5: 60	0.7	0.3	0.5	26.5	0.7	1.5	0.6	2.1	1.3
SJ5: 70	0.7	0.4	0.6	26.3	0.6	1.8	0.6	2.2	1.3
SJ5: 80	0.7	0.3	0.5	26.3	0.7	1.6	0.6	2.2	1.3
SJ5: 90	0.8	0.3	0.5	26.5	0.7	1.3	0.8	1.6	1.2
SJ5: 100	0.7	0.3	0.5	26.5	0.7	1.7	0.6	2.1	1.2
SJ5: 110	0.9	0.8	0.7	25.4	0.4	1.9	0.5	2.0	1.0
SJ5: 120	0.9	0.9	0.7	25.2	0.4	1.8	0.5	1.5	0.8
SJ5: 130	0.9	1.1	0.8	24.7	0.4	1.3	0.8	0.9	0.7
SJ5: 140	0.8	0.4	0.6	26.1	0.6	1.5	0.7	1.6	1.1
SJ5: 150	0.9	0.5	0.6	26.1	0.6	1.9	0.5	2.1	1.1

Sample	C25/(C25+C29)	C23/(C27+C31)	Paq	ACL C17-C35	Pwax	C23/C21	C21/C23	C25/C21	C25/C23
SJ6: 0	0.3	0.1	0.2	29.3	1.1	2.5	0.4	3.4	1.3
SJ6: 10	0.3	0.2	0.2	28.6	1.1	3.4	0.3	4.9	1.5
SJ6: 20	0.5	0.3	0.4	27.8	0.9	3.3	0.3	6.1	1.8
SJ6: 30	0.4	0.2	0.3	28.7	1.0	4.1	0.2	7.1	1.7
SJ6: 40	0.7	0.7	0.5	26.4	0.6	3.0	0.3	3.9	1.3
SJ6: 50	0.8	0.8	0.6	25.8	0.5	3.2	0.3	3.7	1.1
SJ6: 52	0.8	0.7	0.6	26.0	0.5	4.4	0.2	5.8	1.3
SJ6: 56	0.7	0.7	0.5	26.2	0.5	4.0	0.2	5.3	1.3
SJ6: 60	0.8	0.9	0.6	25.8	0.5	2.9	0.3	3.3	1.1
SJ6: 62	0.6	0.5	0.5	26.7	0.6	4.3	0.2	5.8	1.4
SJ6: 66	0.6	0.4	0.4	27.2	0.7	5.6	0.2	4.8	0.8
SJ6: 70	0.5	1.1	0.5	25.3	0.6	3.3	0.3	2.7	0.8
SJ6: 72	0.6	1.4	0.6	25.1	0.5	3.8	0.3	2.7	0.7
SJ6: 76	0.5	0.4	0.4	27.1	0.8	4.3	0.2	4.0	0.9
SJ6: 80	0.5	0.7	0.5	26.4	0.7	3.3	0.3	2.8	0.8
SJ6: 90	0.5	0.6	0.4	26.1	0.7	2.7	0.4	2.3	0.8
SJ6: 98	0.4	0.6	0.4	26.4	0.8	2.1	0.5	1.8	0.8

Triterpenoids

Sample	squaline	taraxer-14-ene	urs-12-ene	taraxast-20-ene
SJ5: 6	-	1	-	-
SJ5: 10	2.7	18.6	-	3.3
SJ5: 20	-	37.4	-	2.1
SJ5: 22	-	78.4	-	6.7
SJ5: 26	-	69.0	2.118735599	57.6
SJ5: 30	31.6	723.1	20.2	475.0
SJ5: 32	3.4	713.9	19.8	386.8
SJ5: 36	-	229.4	5.4	145.8
SJ5: 40	-	59.2	-	50.6
SJ5: 42	-	100.4	-	47.0
SJ5: 46	-	66.9	-	46.2
SJ5: 50	-	8.9	-	-
SJ5: 60	-	5.3	-	-
SJ5: 70	-	3.6	-	1.1
SJ5: 80	-	3.8	-	-
SJ5: 90	-	4.4	-	0.9
SJ5: 100	-	7.3	-	3.3
SJ5: 110	-	-	-	-
SJ5: 120	-	-	-	-
SJ5: 130	-	-	-	-
SJ5: 140	-	-	-	-
SJ5: 150	-	-	-	-

Sample	squaline	taraxer-14-ene	urs-12-ene	taraxast-20-ene
SJ6: 0	48.2	-	-	1.8
SJ6: 10	137.3	3.1	-	-
SJ6: 20	2.5	4.1	-	-
SJ6: 30	2.4	-	-	-
SJ6: 40	3.3	-	-	-
SJ6: 50	3.6	10.3	-	9.6
SJ6: 52	3.6	8.4	-	4.7
SJ6: 56	41.5	-	-	-
SJ6: 60	9.3	2.9	-	2.6
SJ6: 62	23.1	27.1	-	24.8
SJ6: 66	7.9	263.4	10.4	546.5
SJ6: 70	8.0	484.1	20.8	767.6
SJ6: 72	8.7	1053.5	54.1	1805.1
SJ6: 76	3.8	383.7	20.6	755.0
SJ6: 80	10.0	526.6	18.7	745.1
SJ6: 90	7.9	190.5	-	166.3
SJ6: 98	6.6	602.3	20.3	57.9

Concentrations are presented as μg gTOC

Sterols							Stanols		
Sample	phytol	α-tocopherol	brassicasterol	campesterol	stigmasterol	β-sitosterol	campestanol	22E-stigmasterol-22-en-3β-ol	3-stigmastanol
SJ5: 6	488.1	-	80.6	1959.4	1873.2	3065.0	-	-	-
SJ5: 10	287.9	-	31.5	427.1	465.2	1770.2	-	-	115.5
SJ5: 20	176.9	-	26.1	362.3	304.3	1609.8	-	-	92.4
SJ5: 22	185.6	-	42.3	243.7	189.9	2050.1	-	-	146.4
SJ5: 26	94.8	-	21.4	150.9	75.2	2035.8	11.8	-	126.2
SJ5: 30	336.3	-	134.9	596.3	539.7	12073.3	73.4	-	991.1
SJ5: 32	274.3	-	149.0	773.1	652.0	10419.6	136.6	-	959.5
SJ5: 36	718.9	-	138.1	562.1	820.9	4251.1	111.6	88.6	605.4
SJ5: 40	858.0	-	77.0	473.7	700.4	4134.5	136.3	125.3	743.1
SJ5: 42	537.6	-	146.2	874.8	1438.0	6869.6	275.3	164.1	1105.6
SJ5: 46	713.8	-	57.1	374.2	472.9	3245.9	-	65.3	462.7
SJ5: 50	2537.7	-	158.8	984.2	1779.8	8246.0	408.1	233.1	1651.2
SJ5: 60	946.6	-	54.9	507.6	1003.9	3984.2	491.2	103.4	746.4
SJ5: 70	730.6	-	30.3	382.9	840.9	4538.4	203.5	61.7	1046.4
SJ5: 80	322.6	-	7.2	124.1	229.8	751.9	56.7	27.6	187.2
SJ5: 90	606.1	-	-	130.7	226.3	948.7	66.2	61.5	394.1
SJ5: 100	1039.8	-	4.6	112.2	182.2	705.8	96.6	45.0	329.8
SJ5: 110	651.9	-	-	178.0	263.0	1407.7	-	62.7	431.8
SJ5: 120	1241.6	-	38.3	214.2	314.1	1445.4	70.1	62.7	324.7
SJ5: 130	1094.2	-	17.9	107.2	173.3	620.1	14.9	27.3	175.5
SJ5: 140	1675.5	-	23.9	222.7	352.9	1134.8	104.4	77.9	271.0
SJ5: 150	485.5	-	-	179.5	290.1	1153.2	31.1	63.5	307.1

Sample	phytol	α-tocopherol	brassicasterol	campesterol	stigmasterol	β-sitosterol	campestanol	22E-stigmasterol-22-en-3β-ol	3-stigmastanol
SJ6: 0	1031.1	-	428.7	1257.5	1363.7	9863.4	-	-	-
SJ6: 10	397.0	-	481.0	-	738.9	7705.1	-	-	-
SJ6: 20	906.8	-	343.6	862.7	753.4	5262.0	-	-	-
SJ6: 30	783.1	-	246.6	840.9	660.4	5171.0	-	-	-
SJ6: 40	839.0	-	164.4	394.8	580.2	2604.4	-	-	165.8
SJ6: 50	864.6	-	153.6	318.1	610.1	3965.4	99.0	29.5	295.2
SJ6: 52	997.1	-	204.4	375.8	838.5	3930.9	109.3	23.6	368.8
SJ6: 56	1183.2	-	309.6	675.8	1132.2	10309.6	86.3	-	851.2
SJ6: 60	881.5	-	299.2	1282.8	1911.0	5639.8	86.2	-	584.3
SJ6: 62	591.6	-	299.2	1744.0	1943.0	9975.1	186.9	85.5	1108.8
SJ6: 66	213.8	-	92.6	515.4	201.8	6789.6	107.8	28.9	914.4
SJ6: 70	208.0	-	108.9	605.6	277.9	7136.2	295.7	46.4	1198.2
SJ6: 72	299.3	-	232.2	1527.3	891.0	19970.0	596.3	196.3	4082.6
SJ6: 76	360.8	-	140.7	842.6	554.8	8407.8	466.7	116.7	2100.5
SJ6: 80	391.4	146.2	200.2	1448.1	457.6	12314.4	593.6	115.5	2204.7
SJ6: 90	146.2	205.9	67.7	529.2	375.9	6840.8	371.4	99.2	1759.6
SJ6: 98	141.9	55.7	45.0	497.6	267.0	4859.4	291.9	72.0	1360.2

Concentrations are presented as μg gTOC